Talanta 80 (2010) 1932–1938

Contents lists available at ScienceDirect

Talanta

journal homepage: www.elsevier.com/locate/talanta

Wavelength encoded analytical imaging and fiber optic sensing with pH sensitive CdTe quantum dots

César Maule[a,b,c], Helena Gonçalves[a], Conceição Mendonça[a], Paula Sampaio[d], Joaquim C.G. Esteves da Silva[a,*], Pedro Jorge[b]

[a] Centro de Investigação em Química, Departamento de Química, Faculdade de Ciências da Universidade do Porto, Rua Campo Alegre 687, 4169-007 Porto, Portugal
[b] Optoelectronics Unit, INESC Porto, Rua Campo Alegre 687, 4169-007 Porto, Portugal
[c] Departamento de Física, Faculdade de Ciências da Universidade do Porto, Rua Campo Alegre 687, 4169-007 Porto, Portugal
[d] Instituto de Biologia Molecular e Celular (IBMC), Rua Campo Alegre 823, 4150-180 Porto, Portugal

ARTICLE INFO

Article history:
Received 24 July 2009
Received in revised form 14 October 2009
Accepted 23 October 2009
Available online 29 October 2009

Keywords:
Imaging sensors
Fiber optic sensing
Quantum dots
pH sensing
Wavelength encoded

ABSTRACT

CdTe quantum dots (QDs), capped with mercaptopropionic acid (MPA), were synthesized and the variation of their fluorescence properties (steady state and lifetime) with pH was assessed in solution and when immobilized in a sol–gel host. Three different sizes of CdTe QDs with excited state lifetimes ranging from 42 to 48 ns and with emission maximum at 540 nm (QD_{540}), 580 nm (QD_{580}) and 625 nm (QD_{625}) were selected. The solution pH affects the maximum emission wavelength (shifts to higher wavelengths of 23, 24 and 27 nm for QD_{540}, QD_{580} and QD_{625}, respectively), the excited state lifetime and the fluorescence intensity in a reversible way. Linearization of the maximum emission wavelength variation with the pH allows the estimation of an apparent ionization constant (pK_a) for each QD: 6.5 ± 0.1 (QD_{540}), 6.1 ± 0.5 (QD_{580}) and 5.4 ± 0.3 (QD_{625}). The variation of the QDs fluorescence properties was further explored using confocal laser scanning microscopy allowing the implementation of a new calibration method for pH imaging in solution. QDs were successfully immobilized on the tip of an optical fiber by dip-coating using sol–gel procedure. The immobilized QDs showed a similar pH behaviour to the one observed in solution and an apparent lifetime of 80, 68 and 99 ns, respectively. The proposed QDs based methodology can be successfully used to monitor pH using wavelength encoded data in imaging and fiber optic sensing applications.

1. Introduction

Semiconductor nanoparticles, or quantum dots (QDs), are presently a widely used tool in the field of biomedical imaging. In addition, their outstanding luminescent properties make them a very appealing alternative to organic dyes in traditional fluorescence based analytical techniques. Their high photostability and quantum yields, together with the ability to tune their absorption and emission properties, simply by changing the size or composition of the nanoparticles, give them superior performance in many applications [1–3]. For these reasons, in the last few years the use of QDs has been demonstrated in a growing range of chemical and biosensing applications [4–6]. While the majority of these applications has been demonstrated in solution assays, the use of quantum dots in combination with optical fibers and other waveguide platforms is a promising emerging field and an essential step towards the implementation of advanced analytical tools [7].

A necessary condition towards the applications of QDs in biological media is the ability to make them stable in aqueous media. The most common strategies to obtain QDs water soluble involve the modifications of their surface with hydrophilic capping ligands [8,9]. Further functionalization of the QD surface with a given ligand can enable its use as a specific indicator for a variety of analytes [10]. A great diversity of sensing applications has been reported where different capping strategies have been used to detect widely different analytes from a diversity of metallic and non-metallic ions [11,12], gases [13] or explosive molecules [14].

Functionalization of the dots surface with ligands containing ionizable groups can render nanoparticles sensitive to pH. The functionalization of CdSe/ZnS QD with a chromophore whose absorption spectrum shifted according to the surrounding pH has been reported [15]. The absorption shift changed the relative overlap with the QD emission, modulating the fluorescence resonance energy transfer (FRET) efficiency according to the pH. Using this method the authors demonstrated an approximately linear variation of the QD luminescence intensity within the pH range 3–11. A potential problem of this strategy lies in the fact that purely intensity based measurements are prone to be affected by

* Corresponding author.
E-mail address: jcsilva@fc.up.pt (J.C.G. Esteves da Silva).

0039-9140/$ – see front matter © 2009 Elsevier B.V. All rights reserved.
doi:10.1016/j.talanta.2009.10.048

several sources of optical power drift. Although the QD luminescence lifetime was shown to be pH dependent, average values in the order of 15 ns were reported. Therefore the implementation of intensity independent lifetime or frequency domain interrogation techniques would require very fast optoelectronic devices. Other authors implementing similar strategies have used pH sensitive QDs to detect glucose or an avian influenza virus [16,17]. Although the pH sensitivity of CdTe QDs has been studied by many authors [18], in most of the reported applications detection was based in simple intensity quenching measurements, few observations were made on QDs wavelength behaviour.

In a more elaborated approach, a QD based ratiometric probe has been designed [19]. This was achieved by conjugating CdSe/ZnS TOPO overcoated with a NIR luminescent squaraine dye. pH modulated FRET resulted in a luminescent emission displaying an isobestic point at 640 nm, which allowed the implementation of ratiometric detection schemes. The generalization of this approach to sensing different biochemical species is possible because the narrow, size-tunable emission spectrum of QD, acting as donors, can be matched with the acceptor absorption features of an analyte sensitive dye, thereby maximizing FRET efficiency.

In this work, the synthesis of thioglycolate capped CdTe QDs is described and their luminescence properties (excitation and emission wavelengths and lifetimes) obtained as function of the reaction time, concentration and pH presented. It is shown, in a confocal microscopy application, that the spectral behaviour of the QDs with pH enables ratiometric pH imaging without the need of combination with organic indicators. Furthermore, the CdTe QDs were immobilized in sol–gel and their pH sensing properties in fiber optic probes assessed.

2. Experimental

2.1. Reagents

Reagents and the respective percentages of purity were the following: tellurium powder (99.997%); cadmium chloride (99.99%); sodium tetrahydroborate (96%); MPA (99%). Deionized and deoxygenated water was used during the synthesis. Water deoxygenating was accomplished by boiling followed by cooling under nitrogen. An inert nitrogen atmosphere was maintained during the synthesis.

A diluted solution of each QD was prepared in a proportion of 1:25 mL in water. The pH of this diluted solution was reversibly changed in the pH range 4–9 with sodium hydroxide (0.1 M) and hydrogen chloride (0.1 M).

TEOS (tetraethoxysilane) (≥99%), TMOS (tetramethyl orthosilicate) and Ph-TriEOS (phenyltriethoxysilane) were obtained from Sigma–Aldrich Química S.A. (Spain).

2.2. Synthesis of CdTe QD

The QDs synthesis was based on well known previously described work [20–22] with the following particular method: (i) 50 mg of sodium tetrahydroborate were mixed with 2 mL of water followed by 75 mg of tellurium—this solution was left to stabilized for about 24 h; this solution was carefully decanted into 100 mL of water; (ii) 230 mg of cadmium chloride was dissolved in 500 mL of water and mixed with 250 μL of MPA—the pH of this solution was rigorously fixed to 6.5 by the addition of sodium hydroxide 1 M; (iii) the tellurium solution was transferred quickly and vigorously into the cadmium solution and the mixture was refluxed up to 27 h. 50 mL samples were removed at selected reaction times (15, 30, 45, 60, 90, 120 and 180 min, 11, 19 and 27 h) for analysis.

By this method the CdTe nanoparticles were capped with mercaptopropionic acid (MPA) becoming water soluble and pH sensitive. One end of the hydrophilic capping ligands contains a thiol group that binds with the QDs surface. The other polar end contains a carboxylic group that makes them water soluble. Because the carboxylic acid group has acid–base properties the optical fluorescence properties of these QDs can be used as pH sensitive indicators.

To evaluate the behaviour of the QDs when submitted to pH changes, three sets of nanoparticles were selected with peak emission at 540 nm (QD_{540}), 580 nm (QD_{580}) and 625 nm (QD_{625}). The fluorescence measurements were performed during the pH titration of the QDs solution. The titration started at pH 6.3 and small amounts of NaOH (0.1 M) were added until the following pH was achieved. After pH 9, small amounts of HCl (0.1 M) were then added to obtain more acidic solutions down to pH 3.0.

2.3. Preparation of optical fiber probes

Silica optical fibers with core/cladding diameters of respectively 550 and 600 μm were purchased from Thorlabs. The fiber tips were carefully polished and their protective coating removed with acetone followed by rinsing with deionized water. To enhance the efficiencies of excitation and collection of luminescence the fiber tips were reshaped by chemical etching. By slow and controlled immersion (using a step motor) of the tip in 40% HF tapered probes with conical shape were obtained (in a 2 cm fiber length the diameter was reduced from 600 μm to approximately 200 μm). To obtain the luminescent probes the fibers were then dip-coated with the QD-doped sol–gel solutions and left to dry in a clean environment at ambient temperature.

2.4. Immobilization of QD in sol–gel matrix and optical fibers

Two sol–gel preparations were tested for the immobilization of the QDs, one based on TMOS and the other, a hybrid sol–gel, based on TEOS and Ph-TriEOS.

(Sol–gel A—TMOS) TMOS was partially hydrolyzed by mixing with an equal amount of HCl (0.1 M), with vigorous stirring for 2 h at room temperature. The resulting solution became a clear and homogeneous sol–gel. At this point equal amounts of the sol–gel was thoroughly mixed with a water solution of the QD, and poured into 1 cm plastic cells. The sol–gel was left in the dark at room temperature for a day and left to dry in a form of a parallelepiped before making the measurements.

(sol–gel B—TEOS/Ph-TriEOS) 1 mL of TEOS and 50 μL Ph-TriEOS were mixed with 250 μL of hydrogen chloride 0.1 M and shaken for 20 min. 2.50 mL of the raw QD solution was added and the mixture shaken for 5 min. Films were immobilized in glass plates and optical fibers by dip-coating [23].

2.5. Instrumentation

A Spex 3D Spectrofluorimeter with a 75 W xenon lamp and a CCD detector was used. Excitation emission matrices of fluorescence (EEM) were acquired, in an excitation wavelength range from 250 to 550 nm, and in an emission wavelength range from 250 to 710 nm, with a resolution of 5 nm. UV–vis spectra were acquired with a Hewlett-Packard HP8452A diode-array spectrophotometer using 1 cm quartz cells in a wavelength range from 240 to 800 nm with a 2 nm interval and an integration time 0.5 s.

The apparent lifetimes of QD doped solutions and sol–gel membranes were estimated using a frequency domain interrogation set-up. The excitation source was a violet LED, and its current modulated with a function generator (Wavetek) and a voltage/current converter (Analog Modules 775). Silica optical fiber bundles were used to guide the excitation radiation to the samples and also to collect the luminescent emission back to detection which was made

using a silicon photodiode (PDA36A). A lock-in amplifier (SRS844) was then used to evaluate the phase difference between the LED emission and the luminescent signals. By performing a phase scan as function of frequency and fitting the acquired data to well known analytical relations between the phase shift and the modulation frequency [24], the samples average lifetime could be estimated.

Using the same excitation source/fiber bundle combination, the spectral characterization of the solutions and of the sol–gel samples was made using a CCD spectrometer (OceanOptics USB4000).

Confocal microscope images were acquired with a Leica SP2 AOBS SE (Leica Microsystems, Germany). The excitation of QDs was made with the Ar laser lines of 458 and 476 nm. A filter-free prism spectrophotometer head with a set of 3 photomultiplier tubes (PMT) allowed the addressing of distinct detection channels in three user-defined spectral ranges. All the image processing operations were done with MATLAB and ImageJ software [25].

3. Results and discussion

3.1. QD fluorescence properties

Table 1 resumes the photophysical properties of the synthesized QDs. These results show that, considering the relative positions of the absorption and emission peaks, all QDs have relatively large apparent Stokes shifts ranging between 230 and 310 nm. It was also observed that the maximum of the excitation wavelength shows a blue shift of about 30 nm when the concentration of the QDs aqueous solution decreases about ten times—at small dilutions the wavelength is kept almost constant and a marked decrease in the excitation wavelength is observed for dilutions higher than 40% the raw concentration. This result may be explained by the aggregation/disaggregation of the QD or a filter effect.

The emission band and the apparent Stokes shift are sensitive to the reaction time, suffering a deviation for the red and an increase, respectively. The increase in the reaction time leads to a shift of the emission wavelength of the CdTe QDs to longer wavelengths (from yellow/green up to red). Longer reaction times result in bigger nanoparticles and, consequently, to a decrease in the carriers' confinement energy and an increase in emission wavelength. The size of the nanoparticles was estimated using the simple model of Bawendi et al. [26], considering a bandgap energy for bulk CdTe of 1.56 eV [27]. The results shown in Table 1, confirm the increasing size of QD_{540}, QD_{580} and QD_{630} which was approximately 6, 7 and 8 nm, respectively. Therefore, by changing the reaction time the size of the nanoparticles can be adjusted and their emission wavelength tuned. Once the reaction is stopped, the resulting nanoparticles are stabilized in water solutions, showing no significant changes in their spectral properties. Therefore, stable nanoparticles can be obtained with different emission characteristics. In addition, by choosing an appropriate wavelength range, all the nanoparticles can be excited using a single excitation source. The full width of half maximum (FWHM) increases with reaction time (from 42 to 62 nm in the range tested), indicating an increase in the dispersion of the size distribution of the nanoparticles.

Table 1
Photophysical and acid–base properties of CdTe QD.

Property	QD_{540}	QD_{580}	QD_{625}
Excitation wavelength (nm)	307	309	316
Emission wavelength (nm)	540	580	625
Estimated size (nm) [26]	6	7	8
FWHM (nm)	42	44	62
pH sensitivity range (ΔpH)	5.7–8.0	4.6–7.5	3.5–8.1
Variation of the emission wavelength with the pH ($\Delta\lambda_{acid/base}$) (nm)	23	24	27
$\Delta\lambda/\Delta$pH (nm)	9.6	8.3	5.9
pK_a	6.5 ± 0.1	6.1 ± 0.5	5.4 ± 0.3
Variation of the lifetime with the pH ($\Delta\tau_{acid/base}$) (ns)		30–90	
τ_{water} (ns)	42	48	44
$\tau_{sol-gel\ based\ TMOS}$ (ns)	80	68	99

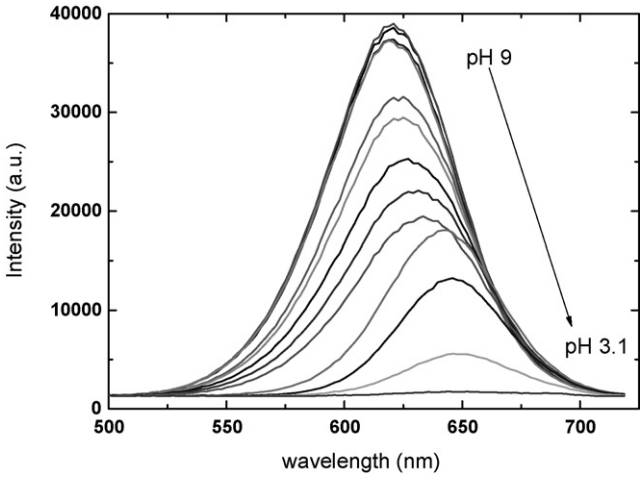

Fig. 1. Emission spectra as function of the pH for QD_{625}.

The emission wavelength of the QDs could be easily tuned between 520 and 630 nm, by increasing the reaction time from 15 min to 27 h. Longer reactions times could result in longer emission wavelengths; however, as the particles grow the effect of quantum confinement starts to decrease, strongly impacting the quantum yield. For smaller nanoparticles the emission efficiency increases with reaction time, however, for reaction times longer than 12 h, the quantum yield decreases. The bandgap energy of bulk CdTe is 1.56 eV [27], which corresponds to an emission wavelength of approximately 795 nm, therefore, to obtain QDs with, longer emission wavelengths different semiconductor materials with smaller bandgap energy must be used (e.g., PbS, PbSe or InAs [28,29]).

The lifetime of the different QDs was also evaluated in water solutions by frequency domain spectroscopy. The decay dynamics of CdTe QD is known to be complex and most often dual or multi-exponential behaviours have been observed. Nevertheless, it is always possible to estimate an average apparent lifetime. The apparent lifetimes of the three QDs were very similar ranging from 42 to 48 ns (Table 1). These values are in agreement with those reported in literature where values ranging from 6 to 125 ns were observed, depending on the QD microenvironment [30,31].

3.2. pH effect on the QD fluorescence properties

The QDs fluorescence intensity, emission spectrum and excited state lifetime in the pH range from 3 to 9 were measured. All QDs exhibited similar behaviour, i.e. as the solution pH was increased, the luminescence intensity increased, the lifetimes decreased and the emission peak was shifted towards shorter wavelengths. The titration procedure was repeated several times, going up and down on the pH scale, and it was observed the changes in the emission peak, the luminescence intensity and the lifetime, were all fully reversible with no observable hysteresis.

Fig. 1 shows an example of the emission spectra variation with the pH of QD_{625}. From this data it can be estimated a wavelength shift of 25 nm for a pH change of 6 units. In the same range the luminescence intensity was quenched by 89%. Similar features were obtained for QD_{540} and QD_{580} and the results are summarized in Table 1.

The presence of a pH dependent wavelength shift suggests that the protonation/deprotonation of the carboxylic ligands of the MPA may influence the QDs bandgap energy. As the pH is increased and the carboxylic ligands ionize, a negatively charged shell builds up in the dots surface that increases the confinement of the charge carriers in the semiconductor core. The increased confinement results in a higher bandgap energy, shorter emission wavelengths and higher quantum yields.

A closer analysis of the data presented in Table 1 reveals that depending on their size, each set of nanoparticles was sensitive to a different pH range. The range of pH sensitivity is 5.7–8.0 for QD_{540}, 4.0–7.0 for QD_{580} and 3.0–8.0 for QD_{625}. The pH dependence of the peak wavelength for the three sets of QDs can be observed in Fig. 2a–c, respectively. Each of the curves obtained are the result of three independent measurements (standard deviation of the average wavelength in each measurement was less than 0.1%), further confirming the reversibility of the changes in the luminescence properties. In addition, these results show that bigger nanoparticles have a pH dependence in an extend range. This happens because, as the average size of particles grows, so does the number of carboxylic ligands on the nanoparticles surface, thereby increasing the number of possible ionization states.

On the other hand, it can also be observed that the shift induced in the emission wavelength is more pronounced for smaller particles. In fact, although the absolute wavelength change increases with particle size, the relative change by pH unit, considering the corresponding sensitive ranges, decreases with growing particle size. This happens because a given change in acidity corresponds to a certain number of ionized carboxylic ligands and the relative change is more pronounced in smaller QDs. In addition, the solutions containing larger nanoparticles have a wider size distribution. This results in a sharper pH response for smaller dots, corresponding to a well defined pK_a and a more broad response for larger QDs, corresponding to a wider pH sensitivity range.

The lifetime of each sample was determined as a function of pH and the corresponding graphical representation is shown in Fig. 3. The analysis of this figure shows that different QDs have different lifetimes, that the lifetime change is relatively small and that this variation occurs in different pH ranges. It can be seen that the lifetime change with pH of bigger QDs has a broader sigmoidal response. This correlates well with the behaviour observed for the wavelength response. In addition, it is also observed that the apparent lifetime decreases as the pH increases. QDs are known to have complex decay dynamics with multi-exponential behaviours. Typically, the shorter lifetime contributions can be attributed to intrinsic recombination of populated core states. Long lived contributions on the other can be associated with the involvement of surface states in the carrier recombination process [32]. Therefore, the behaviour observed could be explained by the increased confinement that enhances the recombination dynamics of surface states. Nevertheless, a more detailed study of the decay dynamics is necessary to better understand the mechanisms involved.

3.3. Confocal microscope imaging

Obtaining analytical information from fluorescent images is a very powerful tool in many applications from biomedical to environmental fields. In particular, self-referenced techniques where the influences of different sources of signal drift are compensated are highly attractive [19,33,34]. If different probes are available, the identification of multiple analytes can be made simultaneously [35]. However, the multiplexing ability of broad emitting organic dyes is quite limited. Therefore, the possibility to use ratiometric analytical imaging methods with the readily multiplexable QDs is highly attractive. To assess the possibility to use these pH sensitive QDs as ratiometric pH probes in imaging applications, different

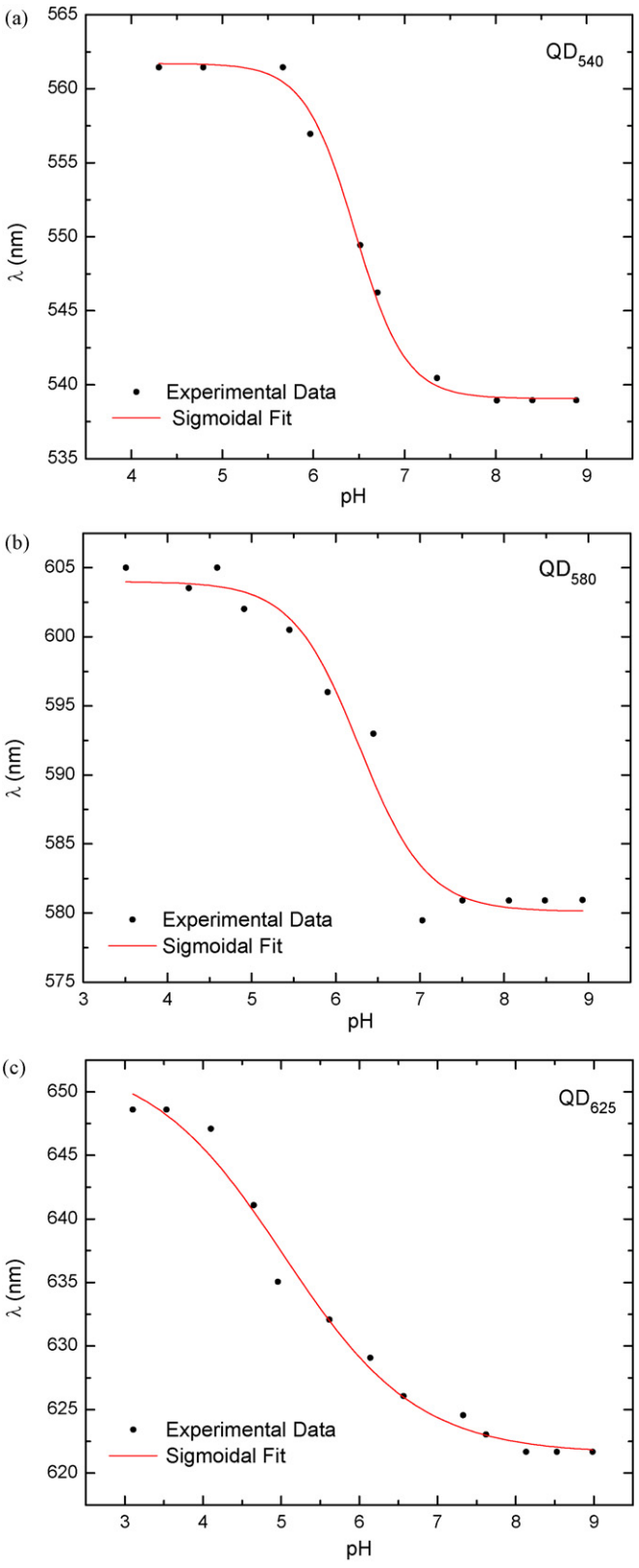

Fig. 2. Variation of the maximum emission wavelength with the solution pH for: (a) QD_{540}; (b) QD_{580}; and (c) QD_{625}. Each curve results from three independent measurements. Standard deviation of measurements is smaller than 0.1%.

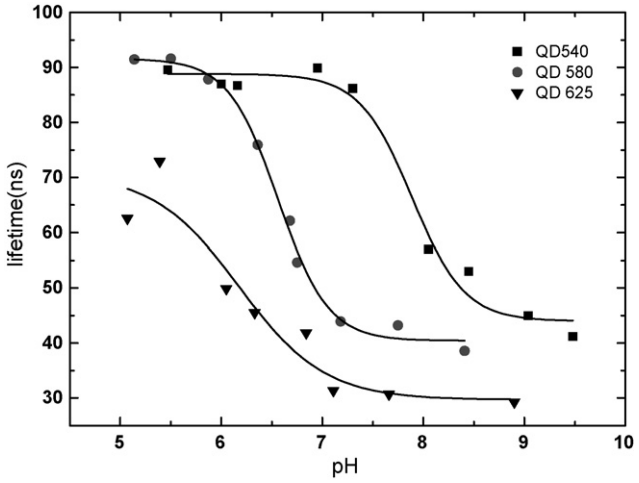

Fig. 3. Dependence of the excited state lifetime with the solution pH.

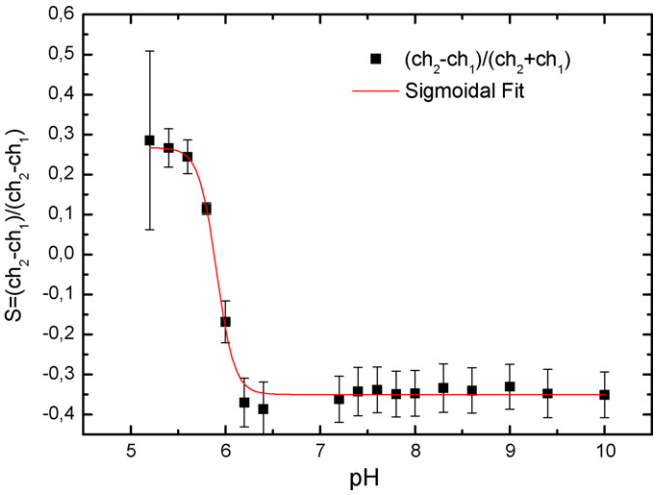

Fig. 4. Ratiometric calibration curve.

buffer solutions doped with pH sensitive QD580 were analysed by confocal laser scanning microscopy.

Using the possibility of the confocal microscope to simultaneously address independent spectral channels a ratiometric detection scheme can be implemented. In particular, if the integrated intensity of two narrow wavelength ranges (channels Ch_1 and Ch_2), chosen in opposite sides of the QDs emission band are recorded, the ratio calculated by $S = (Ch_1 - Ch_2)/(Ch_1 + Ch_2)$ is independent of the intensity and proportional to the wavelength of the emission peak which, in this particular case, is proportional to pH.

This scheme was previously applied for temperature sensing using CdSe–ZnS QDs immobilized in non-hydrolytic sol–gel hosts [36]. This technique can be applied to microscopy by acquiring simultaneously two images of each sample, one through acquisition Ch_1 and another through acquisition Ch_2, each corresponding to the integral of distinct spectral intervals [Ch_1 (540–560 nm) and Ch_2 (620–640 nm)]. By performing the ratiometric scheme described (pixel by pixel), a matrix can then be obtained where each pixel yields a numerical value, given by S, proportional to pH. A false colour scheme can then be applied to obtain images with analytical information.

To calibrate this imaging procedure, several samples corresponding to different pH buffers doped with QDs (ranging from pH 3.2 to 10.0), were analysed. In the pH range between 3.2 and 4.7 the QDs coagulated and precipitated as an orange solid and the images obtained in this pH range were discarded. For the remaining pH range, for each sample, two images with uniform grey level were obtained (one per acquisition channel). The mean value of the grey level intensity (16 bit) of the images was computed, yielding numerical values corresponding to Ch_1 and Ch_2 and ratio S was then calculated. From these operations a sigmoidal calibration curve could be obtained as shown in Fig. 4. In the figure, each data point corresponds to the calculated value of S. The errors bars were calculated considering the standard deviation associated to the values of Ch_1 and Ch_2 and considering error propagation in the calculation of S. The experimental data could be fitted by a four parameter sigmoidal curve with adjusted $R^2 = 0.997$. In the range, pH 5.6–6.2, a linear fit could be obtained with $R^2 = 0.919$.

To demonstrate the feasibility of this method, samples with QDs in different pH buffers were mixed. In particular, a microemulsion was obtained by mixing a few microliters of a QD solution in pH 5.6 and 8 into a drop of silicon oil. Hand shaking of the mixture resulted in a micro-bubbles containing QD solution inside the silica oil droplet.

In Fig. 5, two separate micro-droplets with pH 5.6 (left) and pH 8 (right) are shown. All the images were pre-processed in order to reduce noise (3×3 median filter) and eliminate the non-luminescent background by defining a threshold. The ratiometric scheme and the application of a false colour map using the sigmoidal calibration resulted in images that can be used to estimate the pH. The false colour palette was set between 5 and 6.2 which is the pH range where the wavelength variation took place (all image points with pH higher than 6.2 are represented by the same colour—dark red).

The different stages of the mixing process of two droplets with distinct pH are shown in Fig. 6. The processed images allow seeing clearly that, as the droplets mix, intermediate pH values (between the two extremes 5.4 and 6.2) start to appear. This demonstrates the ability of the ratiometric processing scheme to yield images where a pH value can be ascribe to each pixel.

This technique is therefore promising for pH mapping in bioimaging applications. Similar techniques have been reported using organic dye molecules such as SNARF or phorphyrins (see Ref. [37] and references therein). However, the possibility to implement such analytical imaging techniques using QD introduce several advantages such as increased photostability, narrow emission and tunability of emission wavelength. Such characteristics opens the possibility of using multiple QD probes, each sensitive to a specific analyte (e.g., heavy metals [38,39]), all excited by the same optical source, enabling multianalyte imaging and sensing.

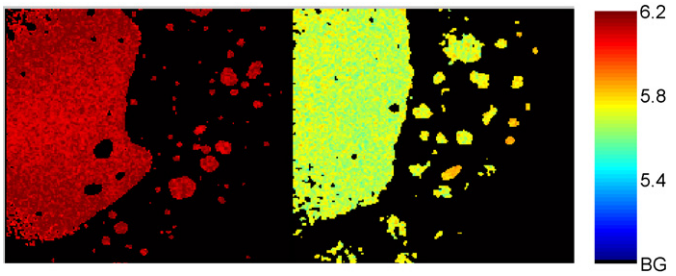

Fig. 5. Image of QDs in pH buffer 5.6 (right) and 8 (left). pH information is given by false colour scale (obtained by application of ratiometric processing and sigmoidal calibration to the original images). Black pixels correspond to background (BG).

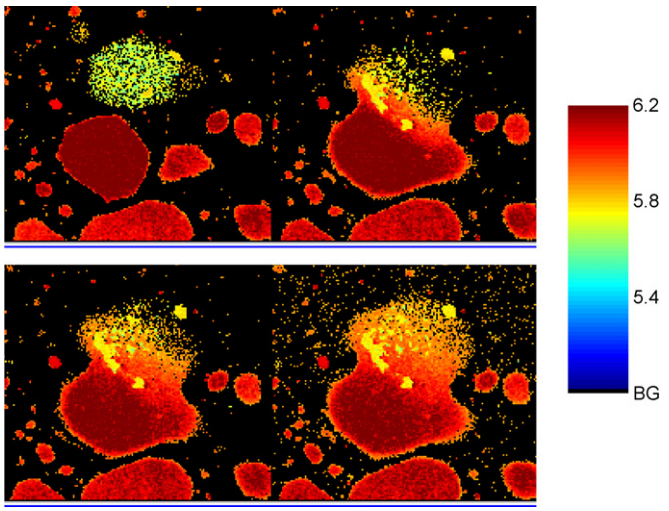

Fig. 6. Sequence of images (from left to right and top to down) showing the mixing process of two droplets with pH values at extremes of the sigmoidal response (8 and 5.6). Black pixels correspond to background (BG).

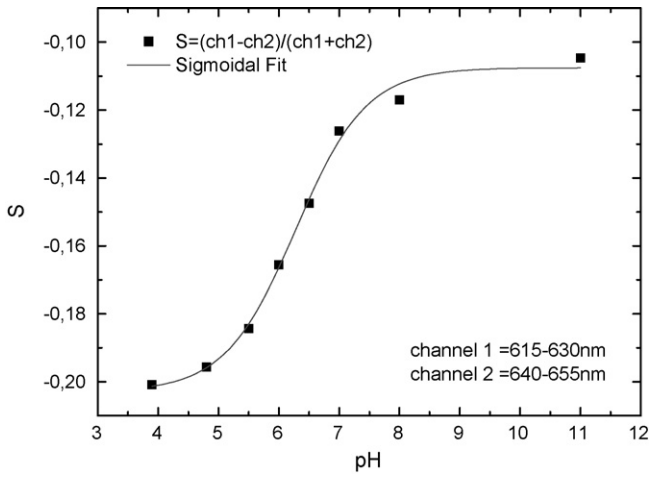

Fig. 7. Ratiometric output of the QD doped fiber probe as function of the solution pH.

3.4. Immobilization of QDs in sol–gel

The QDs were successfully immobilized in TMOS based sol–gel and highly luminescent glass parallelepiped could easily be obtained. The analysis of the emission properties of the monoliths show that the fluorescence intensity of the QDs in the sol–gel based TMOS matrix is enhanced when compared to the one in solutions. This is mostly due to the increase in QDs concentration as a consequence of a volume reduction due to shrinking. Also, the fluorescence emission bands of the different samples are changed from water to sol–gel. All the immobilized QDs showed a shift in their emission peak towards the red, of approximately 14 nm. The immobilization of QDs, introduces changes in their surrounding microenvironment. This is bound to impact mostly their surface states. In particular, the red shift observed indicates that the confinement potential of the immobilized nanoparticles was reduced.

The effect of confinement is also observed in the lifetime behaviour of the QDs. This can be seen in Table 1 where the lifetimes of the QDs in aqueous solutions and in sol–gel matrixes can be compared. In sol–gel the observed lifetimes are higher, by roughly a factor of 2, than those measured in aqueous solutions. The increased lifetimes indicate that the surrounding microenvironment is more favourable to radiative recombination of the long lived surface states when the QDs are immobilized in a sol–gel host. This shows that, while the nanoparticles are very stable in aqueous environments, water may be responsible by partially quenching their luminescence.

When the luminescent glass monoliths entered into contact with different pH aqueous solutions the lifetime and steady state properties of the immobilized QDs did not change significantly and, consequently this sol–gel host was not considered as suitable for sensor applications.

A different immobilization strategy was followed by doping TEOS with Ph-TriEOS. The resulting sol–gel films successfully immobilized the QDs in glass plates and in the tip of optical fibers showing good response to the solution pH. A red shift of approximately 12 nm was observed in the immobilized QDs emission. In this particular case the lifetime was not measured due to reduced signal to noise ratio of the probes obtained. Nevertheless, wavelength ratiometric measurement could be made with the CCD spectrometer.

3.5. Optical fiber probes

The optical fiber probes coated with the TEOS/Ph-TriEOS based films, doped with QD with emission peak at ~635 nm, were tested. When in contact to different pH buffers it could be observed that both luminescence intensity and wavelength were pH dependent, with similar behaviours to the ones observed in solution (Sections 3.2 and 3.3). However, the changes were much smaller indicating that the host matrix had still a significant interference on the QDs behaviour.

In order to evaluate the possibility of using the fiber probes as pH sensors a ratiometric detection scheme, similar to that used above in Section 3.3, was implemented. This scheme was applied to an optical fiber probe doped with QD_{580} setting Ch_1 and Ch_2 for the wavelength intervals of [615, 630 nm], and [640, 655 nm], respectively.

While the wavelength shift observed when the fiber was immersed in pH buffers ranging from pH 4.8 to 11 was barely observable in the spectrometer, it could be easily quantified using the ratiometric scheme. The results obtained are shown in Fig. 7, where the processed output of the fiber probe displays a sigmoidal dependence with pH that is in agreement with the behaviour observed in solution.

These results show the feasibility of pH sensitive QD based optical fiber sensors. However, it was observed that the sensing layer had poor long term stability. The thin film was slowly degrading losing its physical integrity and luminescent capability. This way, although the reversibility of the wavelength response could be observed, a relatively fast degradation of the luminescent intensity was taking place that limited the usefulness of the probes to a small number of essays. Further work is in progress to understand the causes of degradation and to optimize the immobilization procedures.

4. Conclusions

CdTe QDs synthesized and functionalized with MPA were shown to be pH sensitive. The nanoparticles displayed a reversible variation of their peak emission wavelength, emission intensity and lifetime with the pH. The results showed that the emission wavelength changes are more pronounced for smaller particles, which are thus more sensitive to pH. However, it was seen that increasing the particle size lead to sensitivity in a wider range spanning into more acidic pH.

A practical application of these QDs was performed using confocal laser scanning microscopy. A ratiometric scheme was successfully applied to acquired images enabling analytical imaging where pH values could be estimated.

The synthesized QDs were immobilized in different sol–gel hosts. The pH fluorescence behaviour of the nanoparticles immobilized in a TEOS/Ph-TriEOS sol–gel matrix was similar to the one observed in solution. Nevertheless, increased lifetimes and luminescence emission intensities were observed in the solid phase. Also the variations in wavelength and luminescence intensity induced by pH changes were less pronounced in the sol–gel. Nevertheless, it was shown that applying a ratiometric signal processing it was possible to measure pH using a QDs doped optical fiber probe. Work is in progress to improve the long term stability of the fiber probes.

Overall the results obtained show QD as promising labels with analytical capabilities without the need for intermediate indicator dyes and with strong potential for the development of chemically sensitive fluorescent fiber probes. Further functionalization of the quantum dots will enable to apply the same techniques to perform optical fiber sensing or analytical imaging of different chemical analytes, e.g., heavy metals. The use of QDs with different sensitivities together with their multiplexing ability will allow the application of the results obtained in this work in multipoint/multiparameter biochemical sensing and imaging techniques.

Acknowledgements

Financial support from Fundação para a Ciência e Tecnologia (FCT) (Lisboa) (FSE-FEDER) (Projects PTDC/QUI/71001/2006 and POCTI/QUI/44614/2002) is acknowledged. César Maule acknowledges the support from the Marie Curie Early stage research training network, funded by European Commission under the contract MEST-CT-2005-020353. A Ph.D. grant to Helena Gonçalves SFRH/BD/46406/2008 is acknowledged to Fundação para a Ciência e Tecnologia (Lisboa).

References

[1] X.Y. Wu, H.J. Liu, J.Q. Liu, K.N. Haley, J.A. Treadway, J.P. Larson, N.F. Ge, F. Peale, M.P. Bruchez, Nat. Biotechnol. 21 (2003) 41–46.
[2] J.K. Jaiswal, S.M. Simon, Trends Cell Biol. 14 (2004) 497–504.
[3] X. Gao, L. Yang, J.A. Petros, F.F. Marshall, J.W. Simons, S. Nie, Curr. Opin. Biotechnol. 16 (2005) 63–72.
[4] J.M. Costa-Fernandez, R. Pereiro, A. Sanz-Medel, Trac 25 (2006) 207–218.
[5] R.C. Somers, M.G. Bawendi, D.G. Nocera, Chem. Soc. Rev. 36 (2007) 579– 591.
[6] X.X. Wang, M.J. Ruedas-Rama, E.A.H. Hall, Anal. Lett. 40 (2007) 1497–1520.
[7] P. Jorge, M.A. Martins, T. Trindade, J.L. Santos, F. Farahi, Sensors 7 (2007) 3488–3534.
[8] M. Green, H. Harwood, C. Barrowman, P. Rahman, A. Eggeman, F. Festry, P. Dobson, T. Ng, J. Mat. Chem. 17 (2007) 1989–1994.
[9] D. Gerion, F. Pinaud, S.C. Williams, W.J. Parak, D. Zanchet, S. Weiss, A.P. Alivisatos, J. Phys. Chem. B 105 (2001) 8861–8871.
[10] C.J. Murphy, Anal. Chem. 74 (2002) 520A–526A.
[11] Y. Chen, Z. Rosenzweig, Anal. Chem. 74 (2002) 5132–5138.
[12] W.J. Jin, J.M. Costa-Fernandez, R. Pereiro, A. Sanz-Medel, Anal. Chim. Acta 522 (2004) 1–8.
[13] A.Y. Nazzal, L. Qu, X. Peng, M. Xiao, Nano Lett. 3 (2003) 819–822.
[14] G.H. Shi, Z.B. Shang, Y. Wanga, W.J. Jin, T.C. Zhang, Spectrochim. Acta A 70 (2007) 247–252.
[15] M. Tomasulo, I. Yildiz, S.L. Kaanumalle, F.M. Raymo, Langmuir 22 (2006) 10284–10290.
[16] D.B. Cordes, S. Gamsey, B. Singaram, Angew. Chem. Int. Ed. 45 (2006) 3829–3832.
[17] Z. Yun, D. Zhengtao, Y. Jiachang, T. Fangqiong, W. Qun, Anal. Biochem. 364 (2007) 122–127.
[18] A.S. Susha, A.M. Javier, W.J. Parak, A.L. Rogach, Colloids Surf. A 281 (2006) 40–43.
[19] P.T.P.T. Snee, R.C. Somers, G. Nair, J.P. Zimmer, M.G. Bawendi, D.G. Nocera, J. Am. Chem. Soc. 128 (2006) 13320–13321.
[20] J. Huang, K. Sooklal, C.J. Murphy, Chem. Mater. 11 (1999) 3595–3601.
[21] L. Li, H.F. Qian, N.H. Fang, H.C. Ren, J. Lumin. 116 (2006) 59–66.
[22] Z. Deng, Y. Zhang, J. Yue, F. Tang, Q. Wei, J. Phys. Chem. B 111 (2007) 12024–12031.
[23] E.J.E.J. Wang, K.F. Chow, V. Kwan, T. Chin, C. Wong, A. Bocarsly, Anal. Chim. Acta 495 (2003) 45–50.
[24] J.R. Lakowicz, Frequency-Domain Lifetime Measurements in Principles of Fluorescence Spectroscopy, Kluwer-Plenum, New York, 1999, pp. 142–184.
[25] J.B. Sheffield, Microsc. Microanal. 13 (2007) 200–201.
[26] M.G. Bawendi, M.L. Steigerwald, L.E. Brus, Annu. Rev. Phys. Chem. 41 (1990) 477–496.
[27] T. Rajh, O.I. Micic, A.J. Nozik, J. Phys. Chem. 97 (1993) 11999–12003.
[28] E.H. Sargent, Adv. Mater. 17 (2005) 515–522.
[29] L. Levina, W. Sukhovatkin, S. Musikhin, S. Cauchi, R. Nisman, D.P. Bazett-Jones, E.H. Sargent, Adv. Mater. 17 (2005) 1854.
[30] A.M. Kapitonov, A.P. Stupak, S.V. Gaponenko, E.P. Petrov, A.L. Rogach, A. Eychmuller, J. Phys. Chem. B 103 (1999) 10109–10113.
[31] S.F. Wuister, I. Swart, F. van Driel, S.G. Hickey, C.D. Donega, Nano Lett. 3 (2003) 503–507.
[32] S.J. Byrne, S.A. Corr, T.Y. Rakovich, Y.K. Gun'ko, Y.P. Rakovich, J.F. Donegan, S. Mitchell, Y. Volkov, J. Mater. Chem. 16 (2006) 2896–2902.
[33] A. Hakonen, S. Hulth, Anal. Chim. Acta 606 (2008) 63–71.
[34] N. Stromberg, S. Hulth, Anal. Chim. Acta 550 (2005) 61–68.
[35] H.W. Ai, K.L. Hazelwood, M.W. Davidson, R.E. Campbell, Nat. Methods 5 (2008) 401–403.
[36] P.A.S. Jorge, M. Mayeh, R. Benrashid, P. Caldas, J.L. Santos, F. Farahi, Meas. Sci. Technol. 17 (2006) 1032–1038.
[37] T. Leiding, K. Gorecki, T. Kjellman, S.A. Vinogradov, C. Hagerhall, S.P. Arskold, Anal. Biochem. 388 (2009) 296–305.
[38] H.M.R. Gonçalves, C. Mendonça, J.C.G. Esteves da Silva, J. Fluoresc. 19 (2009) 141–149.
[39] J.M.M. Leitão, H.M.R. Gonçalves, C. Mendonça, J.C.G. Esteves da Silva, Anal. Chim. Acta 628 (2008) 143–154.